Chemical Science

EDGE ARTICLE

View Article Online
View Journal | View Issue

Cite this: *Chem. Sci.*, 2017, **8**, 2315

Characterizing aliphatic moieties in hydrocarbons with atomic force microscopy†

Bruno Schuler,*[a] Yunlong Zhang,*[b] Sara Collazos,[c] Shadi Fatayer,[a] Gerhard Meyer,[a] Dolores Pérez,[c] Enrique Guitián,[c] Michael R. Harper,[b] J. Douglas Kushnerick,[b] Diego Peña*[c] and Leo Gross[a]

Received 21st October 2016
Accepted 11th December 2016

DOI: 10.1039/c6sc04698c

www.rsc.org/chemicalscience

We designed and studied hydrocarbon model compounds by high-resolution noncontact atomic force microscopy. In addition to planar polycyclic aromatic moieties, these novel model compounds feature linear alkyl and cycloaliphatic motifs that exist in most hydrocarbon resources – particularly in petroleum asphaltenes and other petroleum fractions – or in lipids in biological samples. We demonstrate successful intact deposition by sublimation of the alkyl-aromatics, and differentiate aliphatic moieties from their aromatic counterparts which were generated from the former by atomic manipulation. The characterization by AFM in combination with atomic manipulation provides clear fingerprints of the aromatic and aliphatic moieties that will facilitate their assignment in *a priori* unknown samples.

Introduction

High resolution atomic force microscopy (AFM) with functionalized tips[1] is evolving towards a valuable tool for molecular structure identification of synthetic[2–5] and natural[6–8] compounds, and products formed by on-surface synthesis[9–16] and atomic manipulation.[2,10,17,18] Structure identification by AFM has the strategic advantage that one can address individual molecules, *i.e.* one can isolate different constituents in a mixture and look at them one by one.[8,9] If enough molecules are imaged, a statistically significant analysis is possible[13] and even rare side products can be identified.[3,19] Moreover, AFM analysis requires only a small amount of material (about 0.1–1 mg)[20] and does not demand the compound to be soluble. Especially the single molecule sensitivity renders AFM an interesting tool for the investigation of complex molecular mixtures like petroleum, which contains a tremendous diversity and number of molecular species,[21,22] of which asphaltenes are one fraction.[8] The compositional complexity of these mixtures is a great scientific challenge with economic relevance in oil production and processing.[23–29] Besides the tremendous diversity of chemical structures in such complex asphaltene mixtures, the poor solubility and difficult volatilization and ionization have considerably impeded their structure elucidation.

AFM is most powerful on planar molecules and much more challenging on non-planar ones. For molecules exhibiting a planar aliphatic hydrocarbon backbone it was demonstrated that a sp^3 and sp^2 hybridized carbon can be distinguished.[2,10] In the present study we investigate molecules with several neighboring tetrahedrally coordinated carbons, resulting in a non-planar carbon backbone and multiple possible adsorption geometries. The low abundance of alkyl and cycloaliphatic moieties and archipelago-type motifs found in a preceding AFM study on asphaltenes[8] has triggered questions whether such molecules can sustain the thermal sublimation step during preparation and be recognized by AFM. This work resolves that issue.

In this work we identified linear and cyclic aliphatic groups in different adsorption geometries and distinguished them from their aromatic planar counterparts that were generated by tip-induced dehydrogenation reactions. The model compounds introduced here have characteristics typical for aliphatic moieties and archipelago-type molecules found in asphaltenes. The alkyl moieties selected span a great enough range to be representative of petroleum. It is demonstrated that the compounds sustain the deposition and can be unambiguously identified by AFM. Identification was based on the AFM contrast on different substrates and by employing atomic manipulation, to: (i) switch the non-planar geometry of aliphatic compounds, and (ii) cleave C–H bonds. We thus show that such molecules can be detected by AFM, and we obtained fingerprints for the identification of aliphatic hydrocarbon moieties, facilitating and improving their chemical identification for future determination of *a priori* unknown molecules by AFM.

[a]*IBM Research – Zurich, Säumerstrasse 4, 8803 Rüschlikon, Switzerland. E-mail: bschuler@lbl.gov*

[b]*ExxonMobil Research and Engineering Company, Annandale, NJ 08801, USA. E-mail: yunlong.zhang@exxonmobil.com*

[c]*Centro de Investigación en Química Biolóxica e Materiais Moleculares (CIQUS), Departamento de Química Orgánica, Universidade de Santiago de Compostela, Santiago de Compostela 15782, Spain. E-mail: diego.pena@usc.es*

† Electronic supplementary information (ESI) available: Additional scanning tunneling microscopy (STM) and atomic force microscopy (AFM) measurements as well as NMR, optical spectroscopy and gas chromatography (GC) characterization of the five model compounds are provided. For CPNP and CHNP the synthetic route is described. See DOI: 10.1039/c6sc04698c

Results and discussion

We investigated a set of five synthetic model compounds featuring aliphatic moieties (see Fig. 1): 1,2-di(pyren-1-yl)ethane (BPE, **1**), 1,10-di(pyren-1-yl)decane (BPD, **2**), 1,20-di(pyren-1-yl) icosane (BPI, **3**), 11,12-dihydro-10*H*-cyclopenta[6,7]naphtho [1,2,3,4-*ghi*]perylene (CPNP, **4**) and 10,11,12,13-tetrahydroanthra [1,2,3,4-*ghi*]perylene (CHNP, **5**). BPE, BPD and BPI were particularly designed to address the linkage between polycyclic aromatic hydrocarbon (PAH) cores, which is the main distinguishing feature between the archipelago and island models of asphaltene structure. CPNP and CHNP comprise cycloaliphatic units. The model molecules introduced here are consistent with asphaltene molecular properties regarding molecular weight, boiling point, H/C ratio and double bond equivalent as reported previously.[30–32]

In Fig. 2a, a scanning tunneling microscopy (STM) overview image of the BPI sample preparation is shown. Even for this comparatively large molecule with a molecular weight of 683 Da and a $C_{20}H_{40}$ aliphatic chain as a linker, the vast majority of the molecules does not dissociate or form aggregates. The two pyrene units of BPI adsorb flat on the substrate and the alkyl chain is typically buckled or twisted. The number of possible conformations of the aliphatic linker increases rapidly with chain length. In Fig. 2b–g AFM images of BPI in a few conformations are shown. Often the typical zig–zag pattern of the alkyl chain lying (partially) flat on the surface can be recognized. Non-planar conformations, that is, sections and twists where the C–C bonds of the alkyl chain are not in a plane parallel to the surface, are more difficult to assign. By providing external stimuli through tip-induced inelastic excitations[33] (Fig. 2h–k) or thermal annealing of the sample to 300 K (Fig. S5†), however, the molecules unbend and preferentially adopt a planar adsorption geometry with an overall straight alkyl chain, suggesting this geometry to be energetically favored on both the Cu and NaCl substrate.

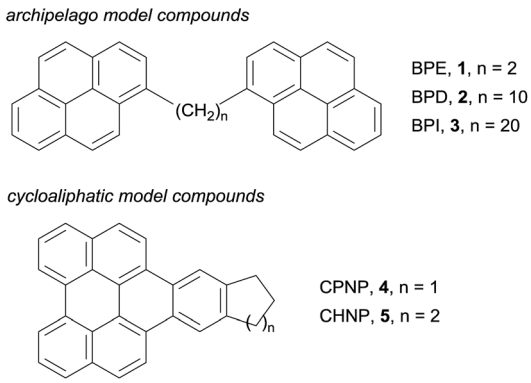

Fig. 1 Model compounds. Chemical structures of the five model molecules.

Similar to BPI, also its smaller analogues BPD and BPE could be deposited intact by fast thermal evaporation, despite the presence of one of the weakest C–C bonds in BPE's aliphatic linker (65.2 kcal mol^{-1}).[34] Because of the generally increasing sublimation temperature with increasing molecular weight, fragmentation will become more problematic for larger molecules. Experiments show that at masses of about 1000 Da, even for completely aromatic PAHs, fragmentation can dominate over intact sublimation,[3] providing an approximate upper bound for molecule deposition by sublimation.

In Fig. 3a–f AFM measurements of BPE, BPD and BPI in the planar conformation at different scan heights are shown. All the methylene units can be clearly identified and differentiated from the sp^2 carbon atoms in pyrene. Because the atoms are not all in the same plane, different scan heights are used for identifying the alkyl chain and the PAH units, respectively (compare upper and lower panels of Fig. 3). The brighter appearance of the alkyl chains compared to the pyrene units indicates the larger adsorption height of the former.[2] In fact, tip induced dehydrogenation[35] to form alkenyl chains significantly reduced

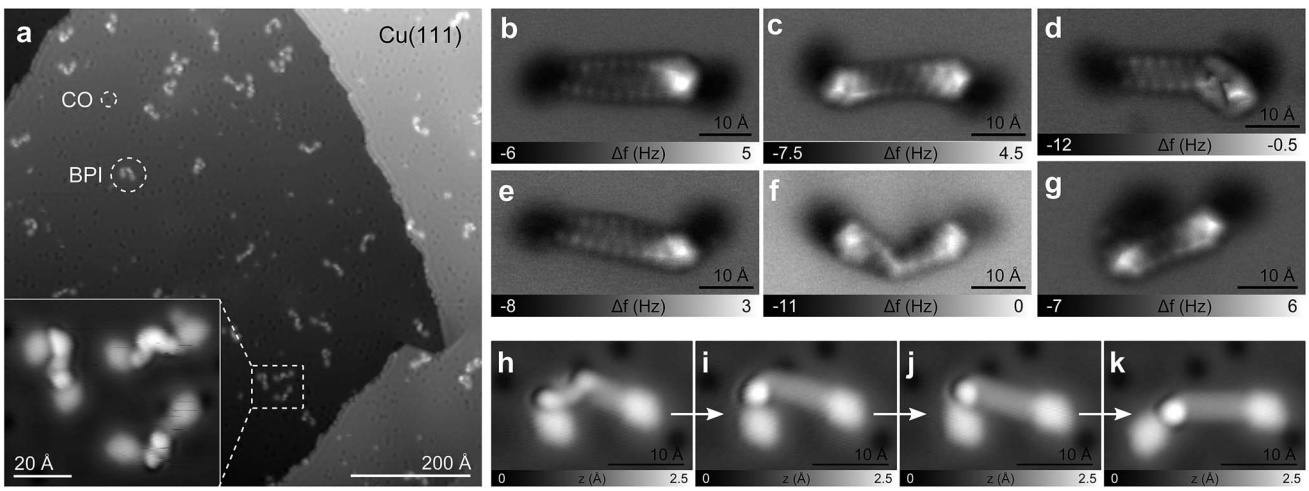

Fig. 2 BPI conformations. (a) STM overview image of the BPI on NaCl(2ML)/Cu(111) sample preparation. Inset shows close-up of three BPI molecules. (b–g) CO tip AFM images of BPI on Cu(111) in different conformations. (h–k) Sequence of STM images ($I = 2$ pA, $V = 0.2$ V) after consecutive tip-induced conformation changes by voltage pulses of $V \approx 3$ V.

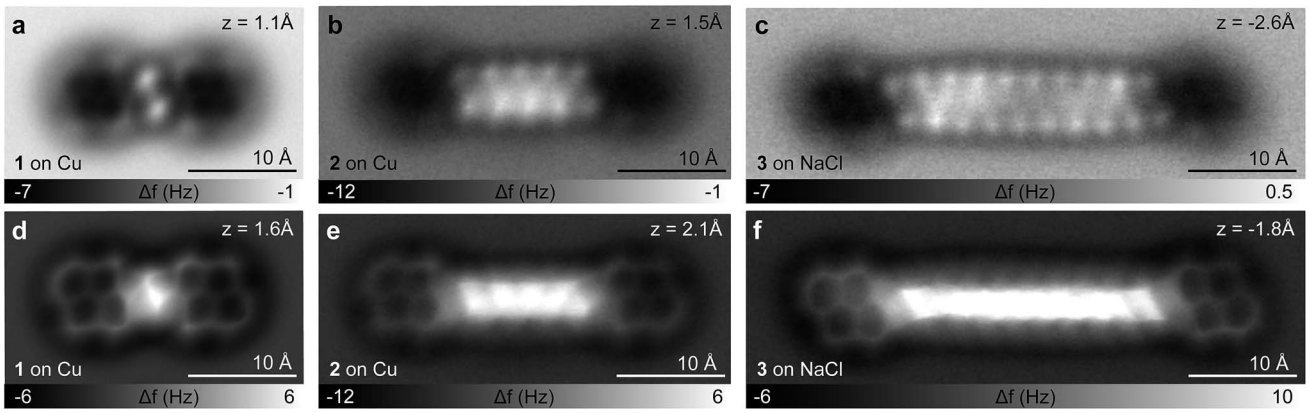

Fig. 3 BPE, BPD and BPI in straight conformation. (a–f) CO tip AFM images of BPE (a, d) and BPD (b, e) on Cu(111) and BPI on NaCl(2ML)/Cu(111) (c, f) at different tip heights.

the adsorption height and thus the brightness of the linker chain (see Fig. 4). Moreover, also the qualitative contrast of alkyl and alkenyl chains is different. In case of the alkyl chains the brightest features are at the rim of the chain corresponding to the apparent location of the protruding hydrogen atoms. Note that there is an apparent increase in width due to the well known effect of CO tip tilting towards the molecule.[36,37] For alkenyl chains the brightest features are in the central part of the chain, above apparent carbon atom positions and carbon–carbon bonds (see Fig. 4). The tip-induced oxidation of the alkyl chain to an alkenyl chain demonstrates (i) the capability to clearly distinguish the two different chains and (ii) the initial integrity of the alkyl chain after deposition. For the more extended alkyl chains even small brightness modulations of the methylene units can be observed, which are probably related to minute differences in adsorption height. For straight alkyl chains the different brightness of methylene units seems to be related to their non-equivalent location with respect to the underlying substrate atoms (see Fig. S2 in the ESI†).

In the BPD and BPI samples we find a low number (<10%) of additional molecules on the surface. Some examples of such molecules are shown in Fig. S9 in the ESI.† The abundance of additional molecules observed is comparable to the impurity content of the material of about 4 wt%, indicating that a significant amount of the deposited additional molecules originate from impurities of the source compound. Although we can exclude fragmentation or chemical transformation of the vast majority of molecules, it cannot be ruled out for a few percent of the BPD and BPI molecules. For the other samples, which were of higher purity, we did not observe additional molecules by AFM.

Besides PAHs and aliphatic chains, other important structural elements in hydrocarbons in general and in asphaltenes in particular are cycloaliphatic moieties. As models for such compounds we synthesized CPNP and CHNP that feature fused cyclopentene and cyclohexene rings, respectively. The CPNP molecule adsorbs differently on Cu and NaCl, showing two adsorption geometries of the same envelope-type conformation (**4a** or **4b**, see Fig. 5). On NaCl, the 5-membered ring adopts an alternating 'up-down-up' geometry (**4a**), meaning that the carbon atoms at the 10 and 12 positions are buckled upwards (increased adsorption height) and the C at the 11

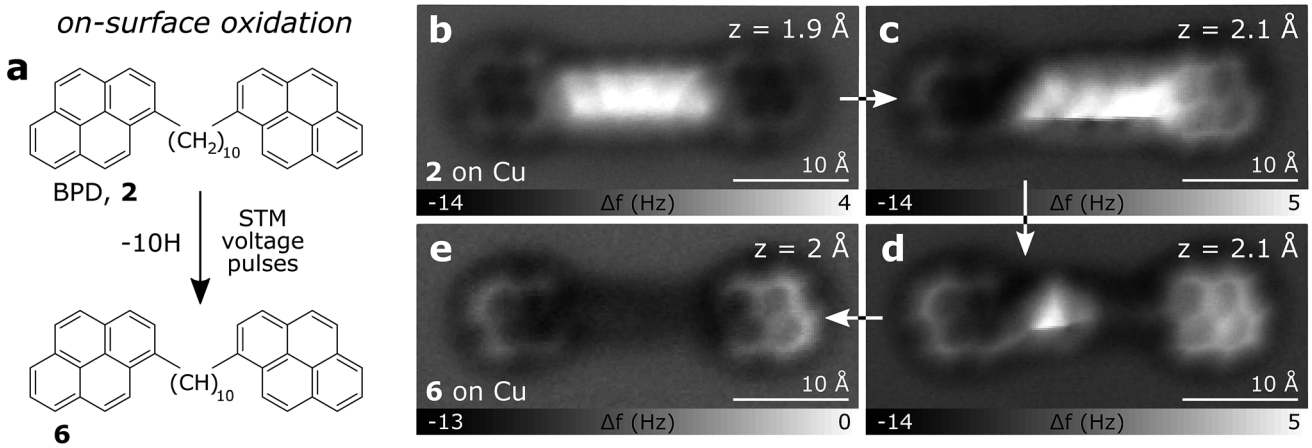

Fig. 4 BPD tip-induced dehydrogenation on Cu. (a) Schematic of the on-surface oxidation process. (b–e) AFM images of BPD on Cu after consecutive tip-induced dehydrogenation of the alkyl chain by several voltage pulses up to 3.5 V.

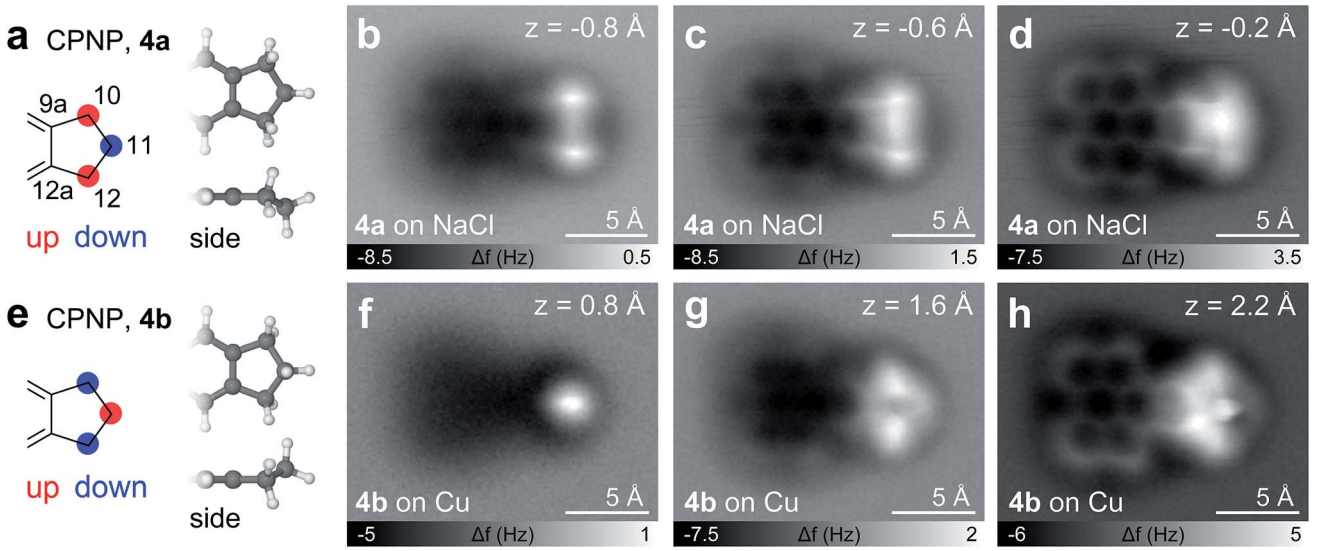

Fig. 5 CPNP, **4**. (a, e) CPNP structure with its two observed adsorption geometries **4a** and **4b**. (b–d and f–h) CO tip AFM images of **4a** (b–d) on NaCl(2ML)/Cu(111) and **4b** (f–h) on Cu(111), respectively, at different tip heights.

position downwards (see Fig. 5e). The assignments of the adsorption geometries are supported by AFM simulations based on the probe particle model by Hapala *et al.*[37] (see Fig. S1†). Note that the apparent bond between the opposing methylene groups in Fig. 5b and c stems from a proximity effect as observed previously.[37–40] On Cu on the other hand, the C in the 11 position buckles upwards to form a 'down-up-down' sequence in the aliphatic ring (**4b**). At close distance (Fig. 5d and h), however, it is unclear whether the native geometry can be fully maintained or whether repulsive tip forces might deflect the atoms from their intrinsic positions. Nonetheless, the cyclopentene moiety can be identified in either adsorption geometry, for both of which we obtained characteristic fingerprints.

Also for CHNP, two different molecular geometries were observed (see Fig. 6 and see Fig. S1† for simulated AFM images). This time, however, they represent the two enantiomers of a chiral half-chair conformation and were found on both, the Cu and NaCl substrate. The cyclohexene moiety adopts an alternating 'down–UP–DOWN–up' (**5a**) or 'up–DOWN–UP–down' (**5b**) geometry, where the degree of deflection is higher for the two carbons at the front of the molecule (positions 11, 12). Again an apparent bond-like feature arises connecting the positions of the two most protruding hydrogen atoms at

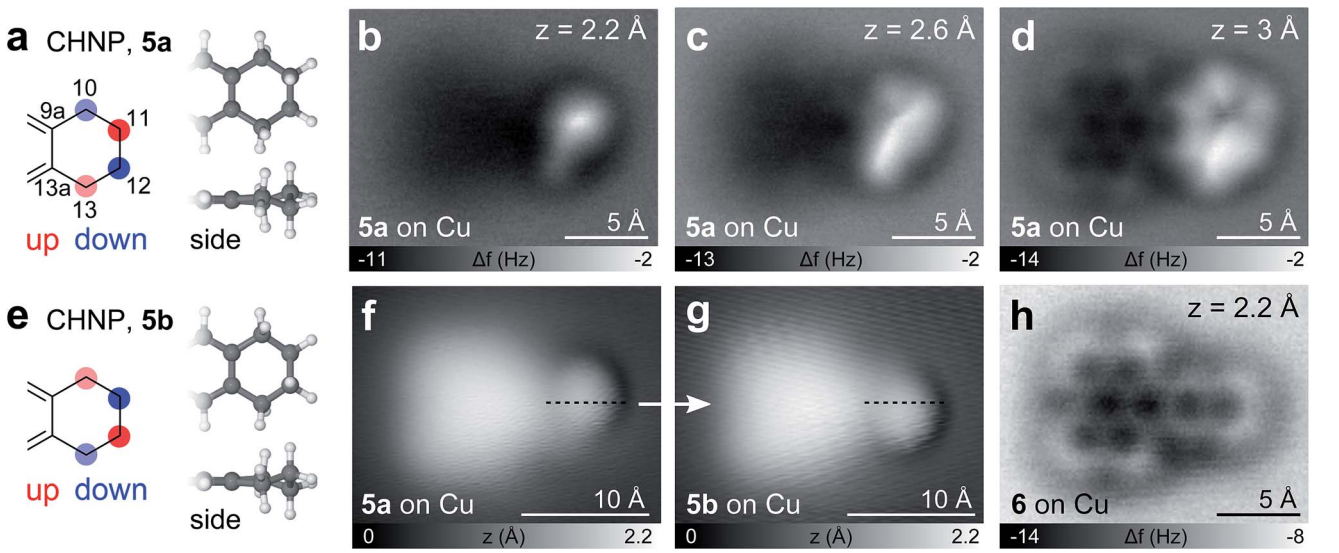

Fig. 6 CHNP, **5**. (a, e) CHNP structure with its two observed enantiomers **5a** and **5b**. The strength of the colored circles indicate the magnitude of the deflection of the C atoms out of planarity. (b–d) CO tip AFM images of **5a** on Cu(111) at different tip heights. (f, g) CO tip STM image of **5a** before (f) and **5b** after (g) enantiomerization with a voltage pulse of $V = -0.4$ V. The dashed line indicates the mirror plane of the transformation. (h) Fully aromatized molecule after removing four H atoms from the aliphatic ring with voltage pulses between 3.1 V and 3.8 V.

positions 11 and 13 of **5a** or positions 10 and 12 of **5b** (most pronounced in Fig. 6c). On both substrates, reversible chiral switching between the two enantiomers[41] could be induced by applying a voltage pulse of $|V| > 0.4$ V in either polarity as shown in Fig. 6f and g.

Like for BPE, BPD and BPI it is also possible to abstract hydrogen atoms from CPNP and CHNP by voltage pulses of about 3.5 V on Cu(111), demonstrating an on-surface oxidation process. In the case of CHNP, the removal of 4H from the cyclohexene group leads to a fully aromatic molecule (see Fig. 6h), reinforcing that the hydrogens did not dissociate during evaporation.

Conclusions

We synthesized and investigated model compounds featuring aliphatic moieties and unambiguously identified them by AFM. All molecules were deposited intact by fast thermal evaporation demonstrating that alkyl chain linkages between multiple aromatic moieties are stable to the preparation process applied for high-resolution AFM. This corroborates the significance of AFM for the structural investigation of complex organic mixtures, and reinforces the higher abundance of island-type asphaltene molecules found in a previous AFM study.[8] By atomic manipulation we accessed different adsorption geometries and oxidized the aliphatic moieties. Using both AFM imaging and atomic manipulation we established fingerprints of alkyl chains and non-planar aliphatic rings in different adsorption geometries for their identification in *a priori* unknown samples.

Methods

STM/AFM experiments

The experiments were performed with a combined STM and AFM in ultrahigh vacuum ($p \approx 10^{-10}$ mbar) and low-temperature ($T \approx 5$ K) using a qPlus sensor.[42] AFM measurements were acquired in the frequency-modulation mode[43] ($f_0 \approx 30$ kHz and $A = 0.5$ Å) at constant-height and zero sample bias. If not stated otherwise, STM measurements were recorded at $I = 2$ pA and $V = 0.2$ V. Tip heights z relate to this tunneling set-point, with $z > 0$ being closer to the substrate. The tip was functionalized with a single CO molecule (referred to as CO tip).[1,44] As a sample we used a Cu(111) single crystal partially covered by islands of bilayer NaCl,[45] denoted as NaCl(2ML)/Cu(111) or simply NaCl. To evaporate the molecules we apply a small grain of the solid material *ex situ* on a (oxidized) Si wafer. In the ultrahigh vacuum this Si wafer is resistively heated to about 900 K within 2 s such that the molecules are evaporated onto the sample, which is held at $T \approx 10$ K. The rapid heating typically enhances the volatility of fragile species.[46,47]

Synthesis

Details on the synthesis of the model compounds and additional characterization can be found in the ESI.†

Author contributions

All authors contributed to the manuscript. B. S., S. F., G. M. and L. G. performed the scanning probe measurements. S. C., D. P., E. G. and D. P. synthesized the CPNP and CHNP molecules. Y. Z. M. R. H. and J. D. K. designed the BPE, BPD and BPI molecules. L. G., B. S., Di. P., Y. Z. and J. D. K. conceived the experiments.

Acknowledgements

We thank Z. Majzik, R. Allenspach and S. P. Rucker for discussions. We acknowledge financial support from the ERC Grants CEMAS (agreement no. 291194) and AMSEL (682144), the EU project PAMS (610446) and the Spanish Ministry of Science and Competitiveness for financial support (MAT2013-46593-C6-6-P).

References

1 L. Gross, F. Mohn, N. Moll, P. Liljeroth and G. Meyer, *Science*, 2009, **325**, 1110–1114.
2 B. Schuler, W. Liu, A. Tkatchenko, N. Moll, G. Meyer, A. Mistry, D. Fox and L. Gross, *Phys. Rev. Lett.*, 2013, **111**, 106103.
3 B. Schuler, S. Collazos, L. Gross, G. Meyer, D. Pérez, E. Guitián and D. Peña, *Angew. Chem., Int. Ed.*, 2014, **53**, 9004–9006.
4 Z. Majzik, A. B. Cuenca, N. Pavliček, N. Miralles, G. Meyer, L. Gross and E. Fernández, *ACS Nano*, 2016, **10**, 5340–5345.
5 N. J. van der Heijden, P. Hapala, J. A. Rombouts, J. van der Lit, D. Smith, P. Mutombo, M. Švec, P. Jelinek and I. Swart, *ACS Nano*, 2016, **10**, 8517–8525.
6 L. Gross, F. Mohn, N. Moll, G. Meyer, R. Ebel, W. M. Abdel-Mageed and M. Jaspars, *Nat. Chem.*, 2010, **2**, 821–825.
7 K. Ø. Hanssen, B. Schuler, A. J. Williams, T. B. Demissie, E. Hansen, J. H. Andersen, J. Svenson, K. Blinov, M. Repisky, F. Mohn, G. Meyer, J.-S. Svendsen, K. Ruud, M. Elyashberg, L. Gross, M. Jaspars and J. Isaksson, *Angew. Chem., Int. Ed.*, 2012, **51**, 12238–12241.
8 B. Schuler, G. Meyer, D. Peña, O. C. Mullins and L. Gross, *J. Am. Chem. Soc.*, 2015, **137**, 9870–9876.
9 D. G. d. Oteyza, P. Gorman, Y.-C. Chen, S. Wickenburg, A. Riss, D. J. Mowbray, G. Etkin, Z. Pedramrazi, H.-Z. Tsai, A. Rubio, M. F. Crommie and F. R. Fischer, *Science*, 2013, **340**, 1434–1437.
10 J. van der Lit, M. P. Boneschanscher, D. Vanmaekelbergh, M. Ijäs, A. Uppstu, M. Ervasti, A. Harju, P. Liljeroth and I. Swart, *Nat. Commun.*, 2013, **4**, 2023.
11 T. Dienel, S. Kawai, H. Söde, X. Feng, K. Müllen, P. Ruffieux, R. Fasel and O. Gröning, *Nano Lett.*, 2015, **15**, 5185–5190.
12 C. Rogers, C. Chen, Z. Pedramrazi, A. A. Omrani, H.-Z. Tsai, H. S. Jung, S. Lin, M. F. Crommie and F. R. Fischer, *Angew. Chem., Int. Ed.*, 2015, **54**, 15143–15146.
13 A. Riss, A. P. Paz, S. Wickenburg, H.-Z. Tsai, D. G. De Oteyza, A. J. Bradley, M. M. Ugeda, P. Gorman, H. S. Jung, M. F. Crommie, A. Rubio and F. R. Fischer, *Nat. Chem.*, 2016, **8**, 678–683.

14 P. Ruffieux, S. Wang, B. Yang, C. Sánchez-Sánchez, J. Liu, T. Dienel, L. Talirz, P. Shinde, C. A. Pignedoli, D. Passerone, *et al.*, *Nature*, 2016, **531**, 489–492.
15 Y. He, M. Garnica, F. Bischoff, J. Ducke, M.-L. Bocquet, M. Batzill, W. Auwärter and J. V. Barth, *Nat. Chem.*, 2016, DOI: 10.1038/nchem.2600.
16 S. Kawai, V. Haapasilta, B. D. Lindner, K. Tahara, P. Spijker, J. A. Buitendijk, R. Pawlak, T. Meier, Y. Tobe, A. S. Foster, *et al.*, *Nat. Commun.*, 2016, **7**, 12711.
17 N. Pavliček, B. Schuler, S. Collazos, N. Moll, D. Pérez, E. Guitián, G. Meyer, D. Peña and L. Gross, *Nat. Chem.*, 2015, **7**, 623–628.
18 B. Schuler, S. Fatayer, F. Mohn, N. Moll, N. Pavliček, G. Meyer, D. Peña and L. Gross, *Nat. Chem.*, 2016, **8**, 220–224.
19 A. Mistry, B. Moreton, B. Schuler, F. Mohn, G. Meyer, L. Gross, A. Williams, P. Scott, G. Costantini and D. J. Fox, *Chem.–Eur. J.*, 2015, **21**, 2011–2018.
20 B. Schuler, F. Mohn, L. Gross, G. Meyer and M. Jaspars, in *Modern NMR Approaches to the Structure Elucidation of Natural Products: Volume 1: Instrumentation and Software*, The Royal Society of Chemistry, 2015, vol. 1, pp. 306–320.
21 K. Qian, R. P. Rodgers, C. L. Hendrickson, M. R. Emmett and A. G. Marshall, *Energy Fuels*, 2001, **15**, 492–498.
22 K. Qian, W. K. Robbins, C. A. Hughey, H. J. Cooper, R. P. Rodgers and A. G. Marshall, *Energy Fuels*, 2001, **15**, 1505–1511.
23 O. C. Mullins, E. Y. Sheu, A. Hammami and A. G. Marshall, *Asphaltenes, Heavy Oils, and Petroleomics*, Springer, New York, 2007, vol. 1.
24 S. Larter, B. Bowler, M. Li, M. Chen, D. Brincat, B. Bennett, K. Noke, P. Donohoe, D. Simmons, M. Kohnen, J. Allan, N. Telnaes and I. Horstad, *Nature*, 1996, **383**, 593–597.
25 R. Quann and S. Jaffe, *Chem. Eng. Sci.*, 1996, **51**, 1615–1635.
26 I. M. Head, D. M. Jones and S. R. Larter, *Nature*, 2003, **426**, 344–352.
27 C. M. Aitken, D. Jones and S. Larter, *Nature*, 2004, **431**, 291–294.
28 J. Ancheyta, F. Trejo and M. S. Rana, *Asphaltenes: Chemical Transformation during Hydroprocessing of Heavy Oils*, CRC Press, Boca Raton, FL, 2010.
29 J. Sheng, *Modern Chemical Enhanced Oil Recovery: Theory and Practice*, Gulf Professional Publishing, Burlington, MA, 2010.
30 A. E. Pomerantz, M. R. Hammond, A. L. Morrow, O. C. Mullins and R. N. Zare, *J. Am. Chem. Soc.*, 2008, **130**, 7216–7217.
31 A. G. Marshall and R. P. Rodgers, *Proc. Natl. Acad. Sci. U. S. A.*, 2008, **105**, 18090–18095.
32 D. C. Podgorski, Y. E. Corilo, L. Nyadong, V. V. Lobodin, B. J. Bythell, W. K. Robbins, A. M. McKenna, A. G. Marshall and R. P. Rodgers, *Energy Fuels*, 2013, **27**, 1268–1276.
33 I. Swart, T. Sonnleitner, J. Niedenführ and J. Repp, *Nano Lett.*, 2012, **12**, 1070–1074.
34 S. J. Blanksby and G. B. Ellison, *Acc. Chem. Res.*, 2003, **36**, 255–263.
35 Y. Kim, T. Komeda and M. Kawai, *Phys. Rev. Lett.*, 2002, **89**, 126104.
36 L. Gross, F. Mohn, N. Moll, B. Schuler, A. Criado, E. Guitián, D. Peña, A. Gourdon and G. Meyer, *Science*, 2012, **337**, 1326–1329.
37 P. Hapala, G. Kichin, C. Wagner, F. S. Tautz, R. Temirov and P. Jelinek, *Phys. Rev. B: Condens. Matter Mater. Phys.*, 2014, **90**, 085421.
38 N. Pavliček, B. Fleury, M. Neu, J. Niedenführ, C. Herranz-Lancho, M. Ruben and J. Repp, *Phys. Rev. Lett.*, 2012, **108**, 086101.
39 A. Sweetman, S. P. Jarvis, H. Sang, I. Lekkas, P. Rahe, Y. Wang, J. Wang, N. R. Champness, L. Kantorovich and P. Moriarty, *Nat. Commun.*, 2014, **5**, 3931.
40 S. K. Hämäläinen, N. van der Heijden, J. van der Lit, S. den Hartog, P. Liljeroth and I. Swart, *Phys. Rev. Lett.*, 2014, **113**, 186102.
41 Y.-S. Fu, J. Schwöbel, S.-W. Hla, A. Dilullo, G. Hoffmann, S. Klyatskaya, M. Ruben and R. Wiesendanger, *Nano Lett.*, 2012, **12**, 3931–3935.
42 F. J. Giessibl, *Appl. Phys. Lett.*, 1998, **73**, 3956.
43 T. R. Albrecht, P. Grütter, D. Horne and D. Rugar, *J. Appl. Phys.*, 1991, **69**, 668.
44 F. Mohn, B. Schuler, L. Gross and G. Meyer, *Appl. Phys. Lett.*, 2013, **102**, 073109.
45 R. Bennewitz, V. Barwich, M. Bammerlin, C. Loppacher, M. Guggisberg, A. Baratoff, E. Meyer and H.-J. Güntherodt, *Surf. Sci.*, 1999, **438**, 289–296.
46 R. Beuhler, E. Flanigan, L. Greene and L. Friedman, *J. Am. Chem. Soc.*, 1974, **96**, 3990–3999.
47 L. Grill, *J. Phys.: Condens. Matter*, 2010, **22**, 084023.